

Engineering a carbon source-responsive promoter for improved biosynthesis in the non-conventional yeast *Kluyveromyces marxianus*

Shane Bassett, Nancy A. Da Silva*

Department of Chemical & Biomolecular Engineering, University of California, Irvine, CA, 92697-2580, USA

ARTICLE INFO

Keywords:
Kluyveromyces marxianus
 Carbon responsive
 Promoter engineering
 Polyketides
 Monoterpene

ABSTRACT

Many desired biobased chemicals exhibit a range of toxicity to microbial cell factories, making industry-level biomanufacturing more challenging. Separating microbial growth and production phases is known to be beneficial for improving production of toxic products. Here, we developed a novel synthetic carbon-responsive promoter for use in the rapidly growing, stress-tolerant yeast *Kluyveromyces marxianus*, by fusing carbon-source responsive elements of the native *ICL1* promoter to the strong *S. cerevisiae* *TDH3* or native *NC1* promoter cores. Two hybrids, *P_{ICL1}350* and *P_{IN450}*, were validated via EGFP fluorescence and demonstrated exceptional strength, partial repression during growth, and late phase activation in glucose- and lactose-based medium, respectively. Expressing the *Gerbera hybrida* 2-pyrone synthase (2-PS) for synthesis of the polyketide triacetic acid lactone (TAL) under the control of *P_{IN450}* increased TAL more than 50% relative to the native *NC1* promoter, and additional promoter engineering further increased TAL titer to 1.39 g/L in tube culture. Expression of the *Penicillium griseofulvum* 6-methylsalicylic acid synthase (6-MSAS) under the control of *P_{IN450}* resulted in a 6.6-fold increase in 6-MSA titer to 1.09 g/L and a simultaneous 1.5-fold increase in cell growth. Finally, we used *P_{IN450}* to express the *Pseudomonas savastanoi* IaaM and IaaH proteins and the *Salvia pomifera* sabinene synthase protein to improve production of the auxin hormone indole-3-acetic acid and the monoterpene sabinene, respectively, both extremely toxic to yeast. The development of carbon-responsive promoters adds to the synthetic biology toolbox and available metabolic engineering strategies for *K. marxianus*, allowing greater control over heterologous protein expression and improved production of toxic metabolites.

1. Introduction

Kluyveromyces marxianus is a non-conventional yeast commonly found in fermented dairy products that demonstrates great potential for industrial applications. *K. marxianus* is both thermal and acid tolerant to temperatures up to and exceeding 50 °C (Lane and Morrissey, 2010) and pH levels as low as 2.0 (Karim et al., 2020), important attributes for preventing cross contamination and reducing cooling costs during cultivation. *K. marxianus* boasts an exceptional doubling time, growing twice as fast as the yeast *Saccharomyces cerevisiae* (Groeneveld et al., 2009), has demonstrated high secretory capacity (Fonseca et al., 2008), and naturally exhibits high flux through the TCA-cycle (Lane and Morrissey, 2010). *K. marxianus* can also assimilate a wide range of carbon feedstocks, including xylose, glycerol, and lactose, matching and even surpassing cell densities from the traditional sugar source glucose (McTaggart et al., 2019). Similar to *S. cerevisiae*, *K. marxianus* has been granted GRAS (generally regarded as safe) and QPS (quality

presumption of safety) status by the U.S. FDA and the European Union, respectively (Ricci et al., 2018).

Recent work has significantly advanced *K. marxianus* for high titer production of chemicals, fuels, and biologics. This includes the development of CRISPR-Cas9 based genome editing systems for single and multigene integrations (Bever et al., 2022; Rajkumar et al., 2019; Li et al., 2021; Löbs et al., 2017), a yeast toolkit of biological parts for synthetic biology in *K. marxianus* (Rajkumar et al., 2019), the development and characterization of native promoter libraries for varying expression (Kumar et al., 2021; Lang et al., 2020; Yang et al., 2015), and full genome-scale and transcriptome-scale probing and engineering efforts to better understand the metabolism of this yeast (Bever-Sneary, 2023; Lertwattanasakul et al., 2015; Li, Mengwan, 2022). These techniques can be used in *K. marxianus* for improved production of acetyl-CoA based products like fatty acids, terpenoids, and polyketides.

Polyketides are a diverse class of natural products that exhibit antimicrobial, anticancer, and immunosuppressive properties, and make up

* Corresponding author.

E-mail address: ndasilva@uci.edu (N.A. Da Silva).

a substantial fraction of all natural product derived drugs approved by the U.S. FDA (Gomes et al., 2013; Pfeifer and Khosla, 2001; Weissman, 2009). Biosynthesis is via specialty enzymes called polyketide synthases (PKS) using CoA metabolites (e.g., acetyl-CoA, malonyl-CoA) as building blocks. Examples of polyketides synthesized at high levels in yeast are the fungal polyketide 6-methylsalicylic acid (6-MSA) using the type I 6-methylsalicylic acid synthase (6-MSAS) from *Penicillium griseofulvum* (formerly *patulum*) (Choi and Da Silva, 2014; Kealey et al., 1998; Wattanachaisaereekul et al., 2007, 2008), and triacetic acid lactone (TAL) using the type III 2-pyrone synthase (2-PS) from the daisy *Gerbera hybrida* (Cardenas and Da Silva, 2014; Markham et al., 2018; Vickery et al., 2018). We previously demonstrated that *K. marxianus* expressing 2-PS (but otherwise unengineered) produced TAL at yields rivaling some of the most extensively engineered *S. cerevisiae* and *Y. lipolytica* strains (McTaggart et al., 2019). Terpenoids are another class of chemicals of significant interest; in particular, monoterpenes are highly sought-after plant natural products with a wide range of commercial applications in fragrances, food flavorings, biofuels, and pharmaceuticals (Zhang et al., 2017). Metabolic engineering of yeasts for the production of terpenoids has primarily focused on improved production of the precursor HMG-CoA for increased flux through the mevalonate pathway (Kampranis and Makris, 2012; Liscum et al., 1985) and on improving production of the precursor geranyl pyrophosphate, which has been shown to be in low availability in *S. cerevisiae* (Jongedijk et al., 2016). Another hindrance to improving synthesis of these classes of products is their cytotoxicity to microbial hosts, including yeast; monoterpenes in particular are exceptionally toxic, with concentrations as low as 0.02%–0.1% v/v resulting in significantly reduced *S. cerevisiae* viability (Brennan et al., 2012; Liu et al., 2022; Zhang et al., 2017).

Carbon responsive promoters are powerful genetic tools for production of toxic chemicals. These promoters are repressed when the carbon source is present followed by transcriptional activation once the carbon source is exhausted (Weinhandl et al., 2014). While such promoters have been identified in conventional organisms like *S. cerevisiae* (e.g., *PA*_{DH2}) (Da Silva and Srikrishnan, 2012; Romanos et al., 1992), *E. coli* (*rpoS*-dependent genes) (Lacour and Landini, 2004), and *Bacillus subtilis* (*Pylb*) (Yu et al., 2015), to date, no such promoters are known in *K. marxianus*. In the closely related *Kluyveromyces lactis*, transcription of the isocitrate lyase-encoding *ICL1* gene was found to be strongly glucose repressed and derepressed by ethanol (López et al., 2004), similar to the *ICL1* function characterized in *S. cerevisiae*. A hybrid *ICL1*-*GAP1* promoter was developed for use in *K. lactis*, taking advantage of the carbon source-responsive elements in *ICL1* for tight repression in glucose combined with *GAP1* for strong expression during stationary phase (Sakhtah et al., 2019).

The development of a *K. marxianus* carbon-responsive promoter for greater stationary phase activation would greatly benefit metabolic engineering strategies in this yeast, especially for production of chemicals toxic to the host. In this study, we designed and evaluated a set of hybrid promoters, using regulatory elements from the native *K. marxianus* *ICL1* promoter, and varying lengths of either the strong constitutive *ScTDH3* or *KmNC1* promoters as the promoter core, for the development of novel carbon-responsive promoters in *K. marxianus*. We identified the strongest hybrid promoters and validated their performance through fluorescence signaling of EGFP. We then produced four compounds of varying toxicity (TAL, 6-MSA, indole-3-acetic acid, and sabinene) and demonstrated that the carbon-responsive promoter resulted in substantially higher production relative to the native constitutive promoter. The use of the carbon-responsive promoter allowed for greater control over heterologous protein expression and improved production of toxic metabolites in this non-conventional yeast.

2. Materials & methods

2.1. Strains and plasmids

All *K. marxianus* strains used were built from base strain CBS712ΔU (McTaggart et al., 2019) or CBS712ΔUΔK (Bever et al., 2022). CBS712ΔUΔH was created by disrupting the *HIS3* locus in strain CBS712ΔU as previously described (Lang et al., 2020). Strain CBS712ΔUΔKΔPGM2-npgA was created by integrating the *P_{ScPGK1}-npgA_{An}-T_{ScCYC1}* cassette into the I4 intergenic site (Rajkumar et al., 2019). The *P_{ScPGK1}-npgA_{An}-T_{ScCYC1}* donor cassette, for expression of the 4'-phosphopantetheinyl transferase npgA from *Aspergillus nidulans* (Lee et al., 2009; Wattanachaisaereekul et al., 2007, 2008), was PCR amplified from plasmid pKD-6MN (primers *ScPGK1p_int* I4.F and *ScCYC1t_int* I4.R) and co-transformed with plasmid pDBtgr-Cas6-I4 (Bever-Sneary, 2023) into CBS712ΔUΔKΔPGM2 (Bever-Sneary, 2023), for Cas9-mediated integrations. Finally, strain CBS712ΔUΔKΔPRB1ΔPGM2-npgA was created by Cas9-mediated disruption of the *PRB1* locus as previously described (Bever-Sneary, 2023). All low copy CEN/ARS plasmids were built from plasmid pIW578 (Lang et al., 2020), high copy plasmids from plasmid pKD-A (McTaggart et al., 2019), and CRISPR plasmids from pDBtgr-Cas9 (Bever et al., 2022). All plasmids and strains are listed in Table S1. Detailed methods for plasmid construction can be found in the Supplemental Information.

Primers are listed in Table S2 and promoter sequences are provided in Table S3. Primers were synthesized by Integrated DNA Technologies (IDT, San Diego, CA). PCR reactions were performed using Q5® Hot Start High-Fidelity DNA Polymerase from New England Biolabs (NEB, Ipswich, MA). Gibson assembly reactions were performed using the NEBuilder® HiFi DNA Assembly Master Mix and all restriction enzymes were from NEB. All plasmids were confirmed by Sanger sequencing or plasmid NGS (Azenta Life Sciences, South Plainfield, NJ) prior to transformation into *K. marxianus*. All genomic modifications were also verified by Sanger sequencing. *K. marxianus* strains were transformed using a modified version of the Frozen-EZ Yeast Transformation II Kit (Zymo Research, Irvine, CA) (Bever et al., 2022).

2.2. Media & cultivation

Escherichia coli strain DH5 α was cultivated in 5 mL of lysogeny broth (LB) containing 150 μ g/mL of ampicillin for molecular cloning and plasmid maintenance. Overnight cultures of *K. marxianus* strains CBS712ΔU or CBS712ΔUΔH were grown in 15 \times 125 mm borosilicate culture tubes containing 3 mL of 2% YPD [10 g/L yeast extract (BD Difco™, Franklin Lakes, NJ), 20 g/L peptone (BD Difco™), and 20 g/L D-glucose (Fisher Scientific, Hampton, NH)] at 30 °C for plasmid transformation. Growth curve and GFP expression experiments were carried out in *K. marxianus* strain CBS712ΔUΔH at 37 °C and 250 rpm in tubes containing 3 mL of the synthetic media 1% SD(-his) or 1% SL(-his) [1.7 g/L yeast nitrogen base without amino acids (BD Difco™), 0.77 g/L CSM-His (Sunrise Science Products, Knoxville, TN), 100 mg/L uracil (Sigma, St. Louis, MO), 5 g/L ammonium sulfate (Fisher Scientific or BD Difco™), and 10 g/L D-glucose or 9.5 g/L lactose (Fisher Scientific), respectively], providing equimolar amounts of carbon. TAL production was in *K. marxianus* strain CBS712ΔU at 37 °C and 250 rpm in tubes containing 3 mL of the synthetic complete SCA media [1.7 g/L yeast nitrogen base without amino acids (BD Difco™), 5 g/L casamino acids (BD Difco™), 5 g/L ammonium sulfate (BD Difco™), and 100 mg/L adenine-hemisulfate (Sigma)] supplemented with lactose (9.5 g/L, 1% SLCA) as the carbon source. 6-MSA synthesis experiments were in *K. marxianus* strain CBS712ΔUΔKΔPRB1ΔPGM2-npgA at 30 °C and 250 rpm in tubes containing 3 mL of the synthetic complete SCA media supplemented with 9.5 g/L lactose (1% SLCA) or 10 g/L xylose (1% SXCA). IAA production was in *K. marxianus* strain CBS712ΔUΔK at 37 °C and 250 rpm in tubes containing 3 mL of the synthetic complete SCA media supplemented with 9.5 g/L lactose and 100 mg/L tryptophan (1%

SLCAT). Sabinene synthesis was in *K. marxianus* strain CBS712ΔUΔK at 30 °C and 250 rpm in tubes containing 3 mL of 1% SLCA or 1% SXCA. Isopropyl myristate (IPM) (Sigma) was added to the culture tubes at 10% of the culture volume for *in situ* extraction, according to a previous protocol (Dusséaux et al., 2020). Absorbance for all cultures was measured at 600 nm using a Shimadzu UV-2450 UV-Vis Spectrophotometer (Shimadzu, Columbia, MD).

2.3. Growth curve measurements

K. marxianus strain CBS712ΔUΔH was individually transformed with pIW578, P_{ScTDH3} -EGFP, and P_{NC1} -EGFP, and plated onto selective 2% SD (-his) plates (2% agar). Biological triplicates from each transformation were streaked onto fresh 2% SD(-his) and 2% SL(-his) plates before inoculation into 3 mL of liquid 1% SD(-his) or 1% SL(-his). Liquid cultures were grown overnight at 37 °C, then reinoculated the next day into their respective liquid media to an $OD_{600} = 0.1$ and grown for 36 h, with OD_{600} readings at hours 2, 4–16 (every hour), 24, 30, and 36, to identify lag phase, early, mid, and late exponential phase, and stationary phase. Maximum specific growth rate (μ_{max}) values were calculated using a minimum of six OD_{600} time points during exponential phase.

2.4. Dynamic EGFP fluorescence

CBS712ΔUΔH was individually transformed with pIW578, P_{ScTDH3} -EGFP, P_{NC1} -EGFP, and the 14 constructed hybrid promoter plasmids, inoculated into 3 mL of liquid 1% SD(-his) or 1% SL(-his) from their respective carbon source plates and grown overnight, and then reinoculated to an $OD_{600} = 0.1$ and grown for 48 h. At each of the five times determined for lag phase, early/mid/late exponential phase, and stationary phase, and at hours 24, 36, and 48, cell culture samples were taken for fluorescence measurements; 20 μ L of each culture was diluted 1:10 and placed in a 96-well black plate, and fluorescence was measured using a SpectraMax M3 plate reader from Molecular Devices (San Jose, CA), with excitation and emission wavelengths of 488 and 511 nm, respectively. Cells transformed with control plasmid pIW578 provided background measurements and all fluorescence units were calculated with background subtracted.

2.5. Metabolite detection assays

For TAL, samples were taken at each time point, centrifuged at 2600 rcf for 5 min to remove cells, and the supernatants collected for TAL analysis by absorbance at 277 nm in the plate reader. TAL samples and standards were diluted at least 1:20 to ensure linearity. 6-MSA was measured using HPLC-UV. Cell culture samples were taken at each time point, centrifuged, and the supernatants collected and diluted 1:2 with ddH₂O. HPLC analysis was conducted using an Agilent 1100 Series Capillary LC System (Agilent, Santa Clara, CA), using a previously described protocol (Choi, 2014). TAL and 6-MSA standards were prepared using pure components purchased from Sigma Aldrich.

For IAA, samples were centrifuged to remove cells and the supernatant diluted 1:4 in ddH₂O. Pure IAA was purchased from Sigma Aldrich for standards. All samples and standards were analyzed using a Shimadzu HPLC system: LC-10AT pumps (Shimadzu), UV-vis detector (SPD-10A VP, Shimadzu), Zorbax SB-C18 reversed-phase column (2.1 × 150 mm, Agilent). Acetonitrile and HPLC grade water each buffered with 1% acetic acid were used as organic and aqueous phases, respectively. A gradient program using a 95–85% Pump B gradient (H₂O with 1% acetic acid) provided an IAA elution time of approximately 24.4 min (flow rate 0.25 mL/min, column temperature 25 °C).

For sabinene, samples were centrifuged to separate the media from the IPM layer, which was decanted into fresh microcentrifuge tubes and centrifuged again to separate any residual aqueous phase. The IPM layer was diluted 1:10 in hexane and transferred to a vial for GC analysis. Sabinene was purchased as an analytic standard (PhytoLab,

Vestenbergsgreuth, Germany) and similarly diluted. All samples and standards were analyzed by GC-FID using an Agilent 6890N GC system with an Agilent DB-WAX column (30 m × 0.25 mm × 0.5 μ m). Helium was used as the carrier gas. The inlet and detector were held at 250 and 300 °C, respectively. 1 μ L of sample was injected with a 2:1 split ratio. The oven temperature was held at 50 °C for 1 min, then increased by 15 °C/min to 120 °C, then increased by 20 °C/min to 230 °C and held for 7 min.

3. Results & discussion

3.1. Carbon source-responsive promoter design through promoter fusions

K. lactis is the closest evolutionary relative to *K. marxianus*, with both yeasts sharing similar properties including the ability to assimilate both glucose and lactose (Lane and Morrissey, 2010; Yu et al., 2021). In *K. lactis*, transcriptional factors Cat8p and Sip4p are regulatory proteins allowing for the glucose repressible expression of *ICL1* (López et al., 2004). Once glucose is exhausted and ethanol production occurs, the *trans*-acting Snf1p/Snf4p kinase complex phosphorylates these two factors and allows them to bind to carbon source-responsive elements (CSREs) in the *ICL1* promoter region, activating transcription (Breunig et al., 2000; López et al., 2004). Given the evolutionary proximity between *K. lactis* and *K. marxianus*, we hypothesized that the glucose repressible mechanism of *ICL1* activation is similar in *K. marxianus*, and that the UAS segment of the *K. marxianus* *ICL1* promoter could be used to regulate heterologous gene expression. Our strategy was to engineer a set of hybrid promoters by fusing the putative carbon source-responsive segment of the native *K. marxianus* *P_{ICL1}* to nested truncation segments of either the *S. cerevisiae* *P_{TDH3}* or the native *K. marxianus* *P_{NC1}*, both of which have shown to be strong promoters in *K. marxianus* (Lang et al., 2020; Yang et al., 2015).

The *K. lactis* *P_{ICL1}* has been confirmed to harbor two CSREs located between nucleotides -811 and -690 upstream of the *ICL1* transcriptional start site, both of which follow the consensus sequence 5'-H SCC WTT NRN SCG R-3', where H = C, A or T; S = G or C; R = A or G; W = A or T; and N = G, C, A, or T (Rodicio et al., 2008). We identified one copy of this same consensus sequence in the 330 bp sequence from -1008 to -678 upstream of the *K. marxianus* *ICL1* transcription start site by comparing the putative promoter sequences between these two yeasts. This *K. marxianus* 330 bp *P_{ICL1}* sequence was isolated from the genomic DNA of strain CBS712ΔU and directly fused upstream of either the *S. cerevisiae* *P_{TDH3}* or the *K. marxianus* *P_{NC1}* promoter sequences, progressively truncated from the 5' end, to create a nested series of hybrid promoters. These fusions started with the full *P_{TDH3}* or *P_{NC1}* sequences, followed by the 500, 450, 400, 350, 250, and 125 bp fragments for a total 14 promoters (four examples shown in Fig. 1). We opted out of using longer fragments as the ~700 bp promoters lead to strong constitutive expression for both *P_{TDH3}* and *P_{NC1}* (Lang et al., 2020). Once fused, the hybrid promoters were individually cloned upstream of the gene EGFP for fluorescence screening.

3.2. Characterizing hybrid promoters for carbon responsive expression of EGFP

We first evaluated growth and EGFP expression using our hybrid promoters in *K. marxianus* strain CBS712ΔUΔH grown at 37 °C in glucose or lactose defined media. Lactose is of interest as we have found superior polyketide synthesis in lactose relative to glucose in this yeast species (Bever et al., 2022; Lang et al., 2020). *K. marxianus* transports lactose into the cell, hydrolyzes the β -linkage, and then assimilates both glucose and galactose simultaneously (noted by a lack of diauxic growth) (Breunig et al., 2000; Fonseca et al., 2013); therefore, we hypothesized that lactose would repress expression from *ICL1* CSRE-containing promoters similar to glucose. To identify optimal sampling times for each phase of growth from these carbon sources,

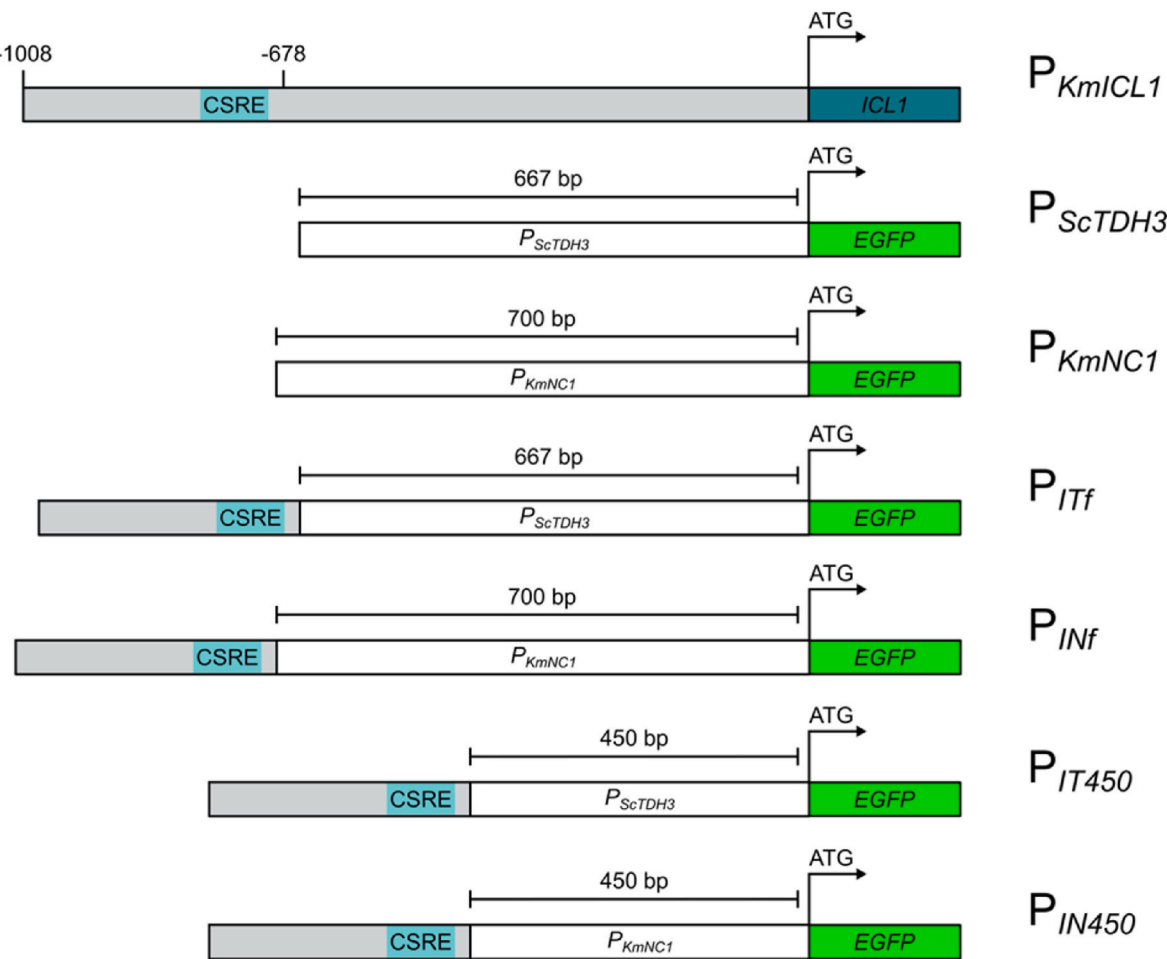


Fig. 1. Design of late phase hybrid promoters in *K. marxianus*. The region upstream of the *KmlCL1* transcriptional start site from nucleotides -1008 to -678 (shown in grey) contains the consensus sequence 5'-H SCC WTT NRN SCG R-3' (teal segment), where H = C, A or T; S = G or C; R = A or G; W = A or T; and N = G, C, A, or T. A series of nested hybrid promoters was created by fusing this 330 bp P_{ICL1} sequence upstream of the *ScTDH3* or *KmNC1* promoters (white) progressively truncating the core promoter sequences from the 5'-end. Shown here are P_{ICL1} , P_{ScTDH3} , and P_{KmNC1} , as well as four of the fourteen hybrid promoters: P_{ITf} , P_{INf} , P_{IT450} , and P_{IN450} . Hybrid promoters were named using the following convention: *I* for *ICL1* sequence, followed by *T* or *N* to designate the promoter core for *TDH3* or *NC1*, finally followed by the truncation length (*f* for full length promoter core, 125–500 for truncated cores).

CBS712ΔUΔH was individually transformed with CEN/ARS control plasmids pIW578, P_{ScTDH3} -EGFP, and P_{NC1} -EGFP, for either no expression or strong constitutive expression. We observed identical growth profiles in all strains across their respective carbon source (Figure S1). Sampling times for fluorescence analysis were chosen as 2, 4, 7, 11, 16, 24, 36, and 48 h post inoculation.

Our hybrid promoters were also individually cloned upstream of the gene EGFP on CEN/ARS low copy plasmids which were transformed into *K. marxianus* strain *CBS712ΔUΔH*. OD₆₀₀ and fluorescence measurements were made at the eight chosen time points, allowing expression to be quantified at all phases of growth. We first evaluated the performance during growth in glucose. Fluorescence across all strains (our set of 14 hybrids and our two unaltered promoter controls) were negligible or statistically insignificant through the first 7 h of growth. By the end of exponential phase (16 h), EGFP expression had reached its maximum for the *S. cerevisiae* P_{TDH3} , with fluorescence approximately 2-fold higher than with P_{NC1} (Figure S2). P_{NC1} was previously characterized as one of the strongest native constitutive promoters tested to date in *K. marxianus* (Lang et al., 2020), so the difference in strength is noteworthy. Our initial screens showed many *ICL1-TDH3* fusions resulted in lower fluorescence than P_{TDH3} at early time points (16 h), and higher fluorescence at later time points (48 h) (Figure S2). Most of the *ICL1-NC1* fusions resulted in similar fluorescence as the unaltered P_{NC1} at 16 h; however, at later time points, higher fluorescence was observed with the fusion

promoters. Of the entire promoter set, P_{IT350} demonstrated the best carbon-responsive activation in glucose medium, with expression favoring stationary phase. This hybrid promoter resulted in lower total and specific fluorescence than the native P_{TDH3} at 16 h, and significantly greater total and specific fluorescence (3-fold, $p < 0.01$) at 48 h (Fig. 2A–B). $NC1$ promoter variants P_{IN500} and P_{IN350} did not demonstrate significant repression at 16 h; however, stationary phase activation was observed with substantially higher fluorescence at 48 h (Figure S2). For all three of these notable promoters, significant increases in fluorescence were only observed once *K. marxianus* was well into stationary phase. P_{IT350} was the most promising in glucose due to both early repression and higher late-phase expression.

We also compared these promoters during growth in lactose medium. We hypothesized that our P_{NC1} -based hybrids would be more responsive in lactose; P_{NC1} regulates the expression of a cell-wall protein (CCW12 homolog) used in lactose transport (Kumar et al., 2021; Lertwattanasakul et al., 2015; Varela et al., 2019). Similar to the glucose studies, OD₆₀₀ and fluorescence measurements were taken at 11-, 16-, 24-, and 36-h post inoculation. In lactose, the unaltered P_{NC1} had peak fluorescence at 24 h, and then a drop in fluorescence between 24 and 36 h (Figure S3). In contrast, $NC1$ promoter variants P_{IN250} , P_{IN350} , and P_{IN450} showed increased fluorescence over this period, with P_{IN450} demonstrating the greatest increase (Figure S3). Total and specific fluorescence from P_{IN450} were lower than for P_{NC1} during exponential

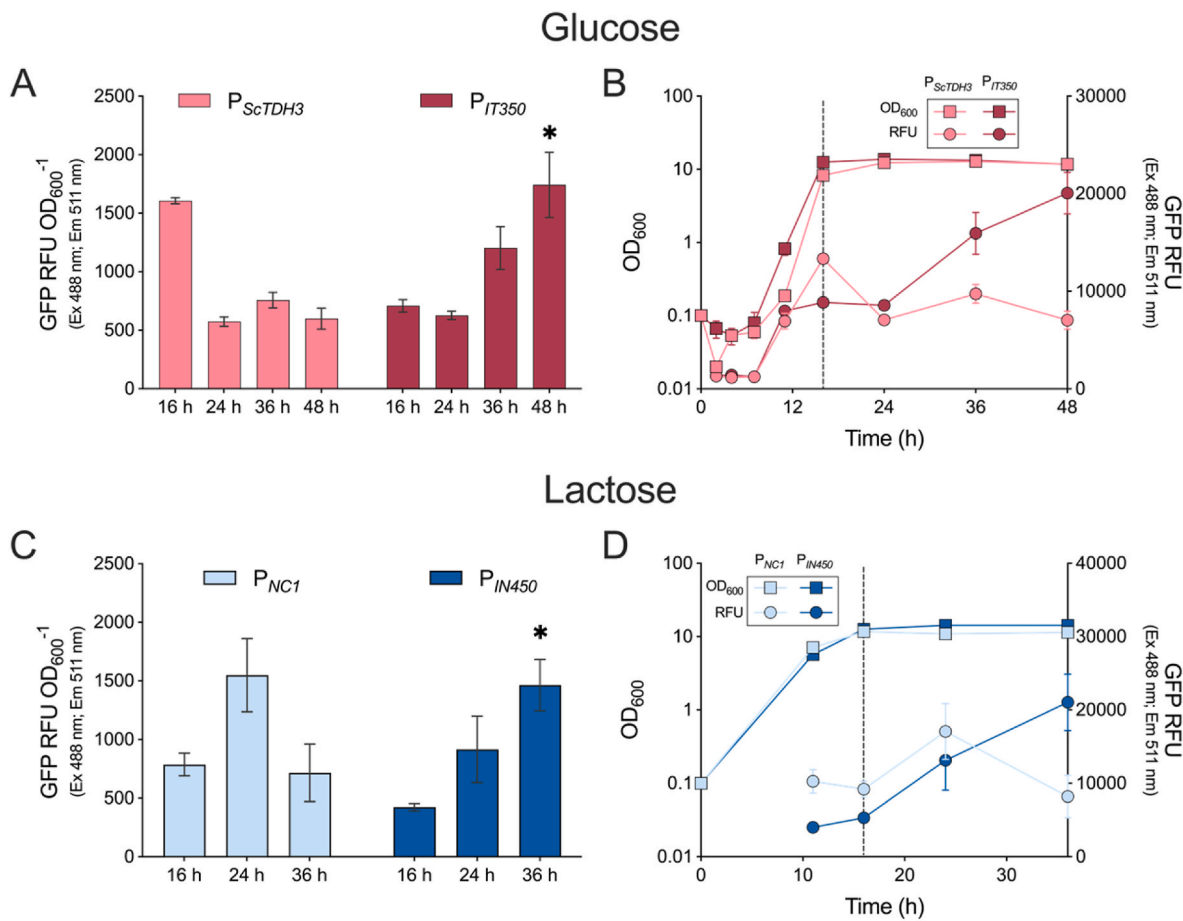


Fig. 2. Carbon-responsive induction of fluorescence in *K. marxianus*. CBS712ΔUΔH harboring plasmids *P_{ScTDH3}*-EGFP (pink), *P_{IT350}*-EGFP (maroon), *P_{NC1}*-EGFP (light blue), or *P_{IN450}*-EGFP (dark blue) was grown in selective glucose (top row) or lactose (bottom row) medium for characterizing expression over time in response to carbon source depletion. (A) Specific fluorescence was compared between the *S. cerevisiae* *P_{TDH3}* and *TDH3* promoter variant *P_{IT350}*, illustrating the strong stationary phase expression using the variant promoter and exponential phase expression using *P_{TDH3}* in glucose medium. (B) Cell densities and relative GFP fluorescence for both *P_{TDH3}* and *P_{IT350}*, confirming an increase in fluorescence by *P_{IT350}* coinciding with stationary phase. (C) Specific fluorescence compared between the native *P_{NC1}* and *NC1* promoter variant *P_{IN450}* confirmed the strong stationary phase expression by the variant promoter in lactose. (D) Cell densities and relative GFP fluorescence shows an increase in fluorescence with *P_{IN450}* coinciding with stationary phase. Due to low fluorescence prior to hour 11, the earlier time points for lactose-based expression were not taken. All fluorescence values (absolute and specific) are normalized to the background fluorescence measured from pIW578. Bars and scatter plots represent mean values \pm one SEM with $n = 3$. * $p < 0.05$ for variants compared against their unaltered counterpart at the respective time point. (For interpretation of the references to colour in this figure legend, the reader is referred to the Web version of this article.)

phase up to 24 h (Fig. 2C–D) indicating repression. By 36 h, total and specific fluorescence from *P_{IN450}* were approximately 2-fold higher ($p < 0.05$) than for the native promoter. In contrast, the *TDH3* promoter variants did not result in the desired behavior and demonstrated the same or similar expression behaviors as the unaltered *P_{TDH3}*, indicative of a lack of regulation in lactose (Figure S3). During growth in lactose, *P_{IN450}* was the most promising promoter, exhibiting partial repression in exponential phase and substantial activation in stationary phase.

3.3. Stationary phase production of the polyketide triacetic acid lactone

In previous work, we achieved high production of the polyketide TAL (Fig. 3A) in an unengineered *K. marxianus* strain grown in xylose or lactose. TAL synthesis from the *Kmpg1* and *Scadh2* promoters was growth-associated, with consistent production of the polyketide throughout exponential growth and minimal changes in TAL titer following the transition to stationary phase (McTaggart et al., 2019). We additionally observed a 50% reduction in growth rate when 1 g/L TAL was added at time zero, indicating TAL to be mildly microstatic to this yeast. For these reasons, we evaluated TAL synthesis using the promising *NC1* hybrid promoters *P_{IN350}* and *P_{IN450}*, with the goal of separating growth and production phases and increasing TAL titers. To best

elucidate the effects of stationary phase activation of 2-PS expression and TAL synthesis, we used multi-copy pKD1-based vectors that result in TAL levels greater than 1 g/L (McTaggart et al., 2019). This previous work also demonstrated significantly higher TAL titer for *K. marxianus* grown in lactose relative to glucose. Therefore, we decided to move forward testing our variants for TAL synthesis during growth in lactose only.

The 2-PS gene was cloned downstream of *P_{NC1}*, *P_{IN450}*, or *P_{IN350}* on multi-copy pKD1-based plasmids, individually transformed into CBS712ΔU, and grown for 48 h in lactose, with sampling at 11-, 16-, 24-, 36-, and 48-h post inoculation. Both *P_{IN450}* and *P_{IN350}* exhibited stationary phase activation for 2-PS expression and TAL synthesis, reaching TAL titers greater than 1 g/L, over 50% higher than the maximum titers from *P_{NC1}* ($p < 0.01$). With *P_{IN450}*, titer reached $\sim 1.2 \pm 0.1$ g/L (Fig. 3B) and yield was 0.029 mol TAL/mol C, significantly outcompeting our previously observed best titer and yield in lactose (Bever et al., 2022). The specific titer (Fig. 3C) indicated late phase activation; with *P_{IN450}*, specific TAL was significantly lower than the native promoter at 11 h and substantially higher at 36 and 48 h. Final cell densities were not significantly different across the three promoters, but growth rate was slower with *P_{NC1}* compared to the two hybrid promoters (Figure S4). We also tested a 450 bp truncation of the *NC1* promoter without the

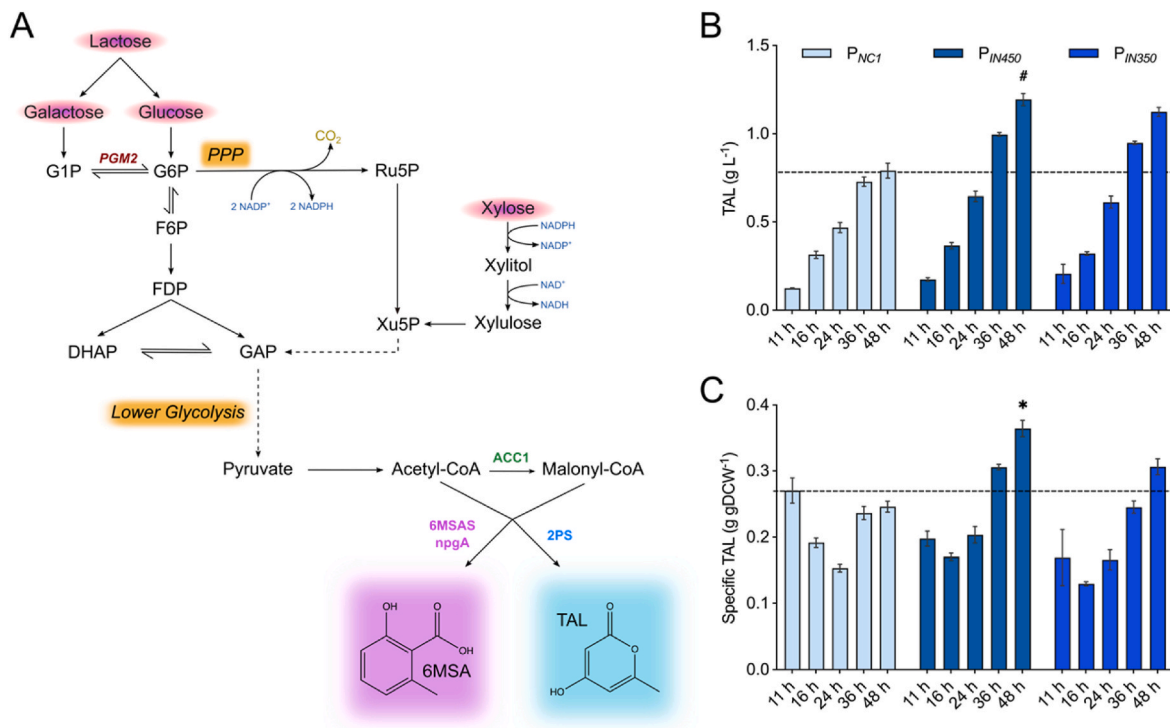


Fig. 3. TAL synthesis in lactose from carbon-responsive promoters. (A) Simplified pathway schematic for polyketide biosynthesis in *K. marxianus* from lactose and xylose assimilation. (B) Absolute TAL titers and (C) specific TAL titers were measured at 11-, 16-, 24-, 36-, and 48-h post inoculation for *P_{NC1}*, *P_{IN450}*, and *P_{IN350}* expressing 2-PS in CBS712ΔU. Both *P_{IN450}* and *P_{IN350}* result in titers greater than the unengineered *NC1* promoter. Bars represent mean values \pm one SEM with $n = 3$, $*p < 0.01$, $**p < 0.001$, where statistical analysis was performed against *NC1* at the respective time point.

regulatory *ICL1* element upstream and saw no changes in growth or TAL synthesis (Figure S5), indicating that both the improved strength and responsiveness of *P_{IN450}* comes from the fusion with the *ICL1* UAS. We concluded that promoter *P_{IN450}* was our best carbon-responsive promoter for 2-PS expression and TAL production, with lower synthesis during exponential phase and increased expression following the transition to and throughout stationary phase, resulting in one of our highest ever TAL titers and yields from *K. marxianus*.

3.4. Promoter engineering to improve carbon responsiveness and polyketide biosynthesis

While specific TAL titer was lower at 11 and 16 h for *P_{IN450}* relative to the native *P_{NC1}*, even tighter control is desired. The *K. lactis* *ICL1* contains two CSRE sequences for carbon-based repression; the *K. marxianus* *ICL1* contains only one CSRE sequence. Therefore, to potentially increase the carbon repressibility of our hybrid *K. marxianus* promoter, we added a second CSRE consensus sequence 66 bp upstream of the first by site-directed mutagenesis (Fig. 4A), following the same design observed in the native *K. lactis* sequence. We inserted the resulting promoter (*P_{IN450v2}*) upstream of the 2-PS gene on a multi-copy pKD1 plasmid, transformed the plasmid into strain CBS712ΔU, and evaluated the expression profile for cultures grown in 1% lactose medium. Given the additional carbon repressible motif, we anticipated tighter regulation of 2-PS expression during exponential and early stationary phase, and therefore stronger derepression and expression in stationary phase.

We first considered promoter strength and compared TAL titers at 48 h. Absolute TAL using *P_{IN450v2}* was 19% higher than with *P_{IN450}* ($p < 0.05$) and 76% higher than with the native *P_{NC1}* ($p < 0.01$) (Fig. 4B), indicating promoter engineering had improved the strength of this hybrid promoter. We then considered repressibility during exponential phase following the same time course of 11–48 h. For *P_{NC1}*, specific TAL decreased over the first 24 h (similar to Fig. 3C), indicating TAL synthesis lagged relative to cell growth. Following the transition to

stationary phase, production levels did increase, but did not rise above the initial level observed at 11 h (Fig. 4C). For both *P_{IN450}* and *P_{IN450v2}*, specific TAL levels showed little change throughout the first 24 h, followed by a substantial increase from 24 to 48 h (Fig. 4C). This increase was greater for *P_{IN450v2}*, demonstrating better stationary phase activation. However, the addition of a second CSRE did not mitigate leaky behavior as specific titers through the first 24 h were higher than those for *P_{IN450}*. This finding supports the claim that CSREs play a greater role in starting transcription rather than preventing it, and the more CSREs present, the greater the expression rate once the carbon source is exhausted and the involved transcription factors can bind (López et al., 2004). Despite this, our second-generation hybrid promoter further improved TAL synthesis in *K. marxianus*, reaching a titer of 1.39 g/L.

3.5. Carbon source-dependent promoter behavior for production of the polyketide 6-MSA

The polyketide 6-methylsalicylic acid (6-MSA) is synthesized through three iterative condensations of malonyl-CoA onto an acetyl-CoA that remains bound to an acyl carrier protein domain (Hitschler and Boles, 2019) of the *P. griseofulvum* 6-methylsalicylic acid synthase (6-MSAS) (Fig. 3A) (Kealey et al., 1998). 6-MSAS also requires a 4'-phosphopantetheinyl transferase (PPTase) for proper post-translational modification and PKS activation. This polyketide is even more toxic to *K. marxianus* than TAL; growth rates are significantly impaired with the addition of as little as 0.5 g/L 6-MSA, and growth is fully inhibited at 1 g/L (Bever-Sneary, 2023). We thus evaluated the more repressible carbon responsive promoter (*P_{IN450}*) for improving production of 6-MSA.

The 6-MSAS coding sequence was cloned downstream of *P_{NC1}* or *P_{IN450}* on a multi-copy pKD1 plasmid. The *A. nidulans* *npgA* PPTase expression cassette was integrated into strain CBS712ΔUΔKΔPGM2, containing a *PGM2* knockout. This gene encodes a phosphoglucomutase, used for diverting carbon flux from glycolysis to glycogen storage; we

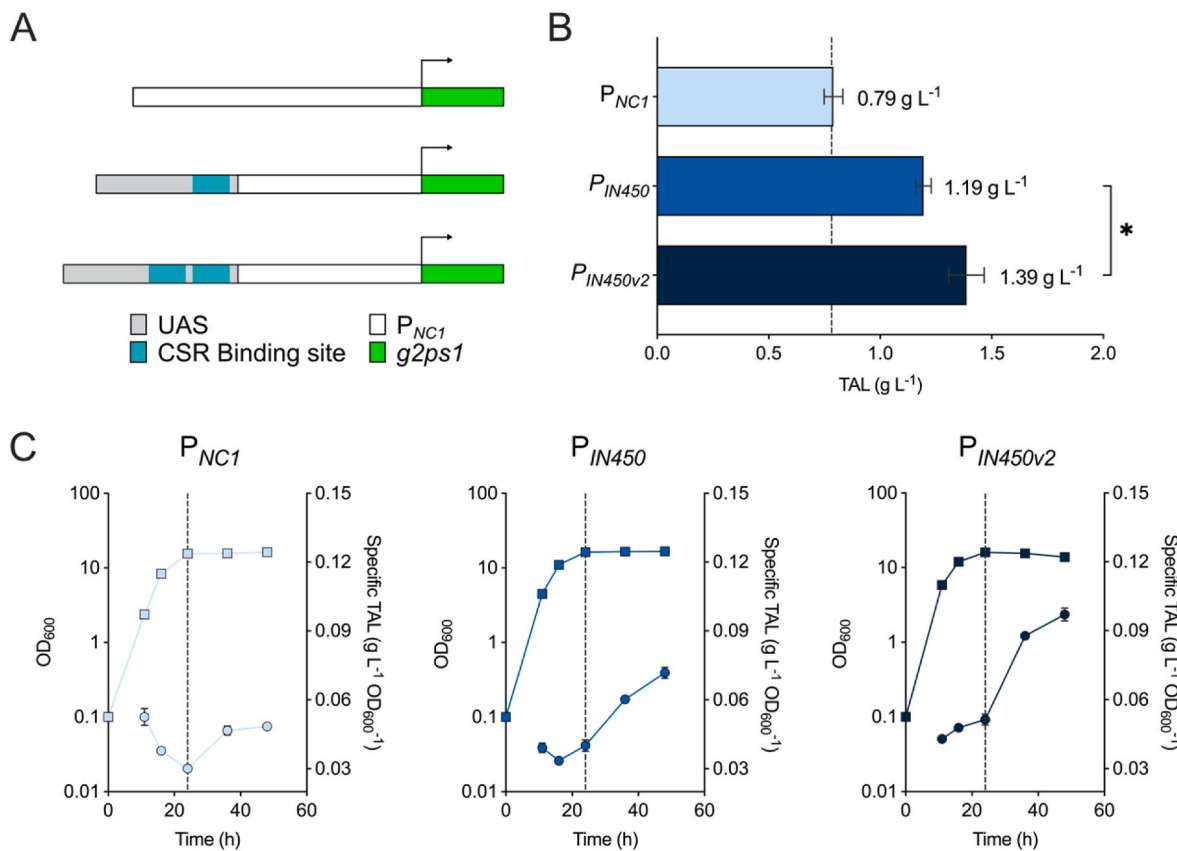


Fig. 4. Rational promoter engineering leads to greater strength and increased stationary phase expression. (A) Schematic of engineering our hybrid promoter by adding a second CSRE site upstream of the original, following the promoter architecture of the *ICL1* promoter in *K. lactis*. (B) CBS712Δ*U*, transformed with pKD-N2PS, pKD-IN450-2PS, or pKD-IN450v2-2PS, was cultured for 48 h in selective lactose media. $P_{IN450v2}$, rationally engineered to contain two CSREs, demonstrated the greatest absolute titers after 48 h, indicating stronger promoter strength. (C) Time course studies with these three promoters revealed that $P_{IN450v2}$ maintains specific TAL titers through the first 24 h, with a substantial increase in specific titer only at 36 h. Bars and scatter plots represent mean values \pm one SEM, $n = 3$, $*p < 0.05$. Scatter plot square points represent OD₆₀₀ values and circular points represent specific TAL titers at the 11, 16, 24, 36, and 48 h time points.

previously found the deletion of *PGM2* improves polyketide synthesis in both *K. marxianus* and *S. cerevisiae* as this limits competing glycogen formation (Bever-Sneary, 2023; Cardenas and Da Silva, 2014). We also previously showed that 6-MSAS is highly susceptible to protease degradation in *K. marxianus* (Bever-Sneary, 2023); because 6-MSAS is susceptible to vacuolar degradation (Spencer and Jordan, 1992), we disrupted the vacuolar protease *PRB1* gene to create CBS712Δ*U*Δ*KΔPRB1ΔPGM2-npgA*. Finally, a previous study found that the thermal stability of 6-MSAS is significantly impacted at 37 °C compared to the native 25 °C for *P. griseofulvum* (Light, 1967). We also observed significantly higher 6-MSAS titers with *K. marxianus* grown at 30 °C compared to 37 °C (Bever-Sneary, 2023), and therefore opted for growth at 30 °C.

We assessed both the strength and carbon-responsiveness of the hybrid promoter by sampling over time through 48 h. Cell densities were higher at all time points for P_{IN450} relative to P_{NC1} , and 47% higher at 48 h (Fig. 5A). 6-MSA is significantly more toxic to *K. marxianus* than TAL, so the increase in growth when using our hybrid promoter is noteworthy. 6-MSA titer was also substantially higher with P_{IN450} , reaching 1.09 g/L 6-MSA. This is a 6.6-fold increase over that with the native promoter (Fig. 5B) and the highest 6-MSA titer to date from *K. marxianus*, significantly surpassing 6-MSA titers from our previous metabolic engineering studies with this yeast (Bever-Sneary, 2023). 6-MSA levels were quite low (<100 mg/L) through the first 16 h with P_{IN450} , with a noticeable increase at 24 h followed by a sharp increase at 36 h. Specific 6-MSA levels provide a better understanding of the underlying behavior. With P_{NC1} , specific titer decreases throughout the 48 h; however, with P_{IN450} specific production is constant for the first 24 h,

followed by a sharp increase by 36 h (Fig. 5C). Similar to TAL production, this substantial increase in 6-MSA synthesis coincided with the transition to stationary phase, and thus indicated stationary phase activation.

Our primary interest was synthesis in lactose medium where P_{IN450} functions as a carbon-responsive promoter. We do not expect similar control in xylose for a promoter with a CSRE; however, we also evaluated promoter behavior in xylose medium for comparison, as substantial increases in TAL are generally seen with this sugar relative to lactose (McTaggart et al., 2019). During the 48 h time course (Fig. 5), growth and absolute titers were also greater at all time points with P_{IN450} , with a 2.5-fold increase in TAL titer relative to P_{NC1} at 48 h. However, carbon-responsive behavior was not observed; both P_{NC1} and P_{IN450} have nearly identical specific 6-MSA profiles (Fig. 5F). This confirms that the CSRE is not effective, that P_{IN450} can act as a strong growth-associated promoter in xylose, and that the promoter is effective at significantly increasing production of this metabolite in both sugar sources.

3.6. Carbon responsive promoter expression improves production of two highly cytotoxic compounds

K. marxianus has demonstrated the ability to be a powerful microbial cell factory. The TAL yields corresponding to the titers in Figs. 3 and 4 meet or exceed many previously reported from extensively engineered *S. cerevisiae* and *Y. lipolytica* strains during batch fermentation (Cardenas and Da Silva, 2014; Markham et al., 2018; Yu et al., 2018). To broaden our product range, we next evaluated production of two highly cytotoxic metabolites that are important to the agriculture and pharmaceuticals &

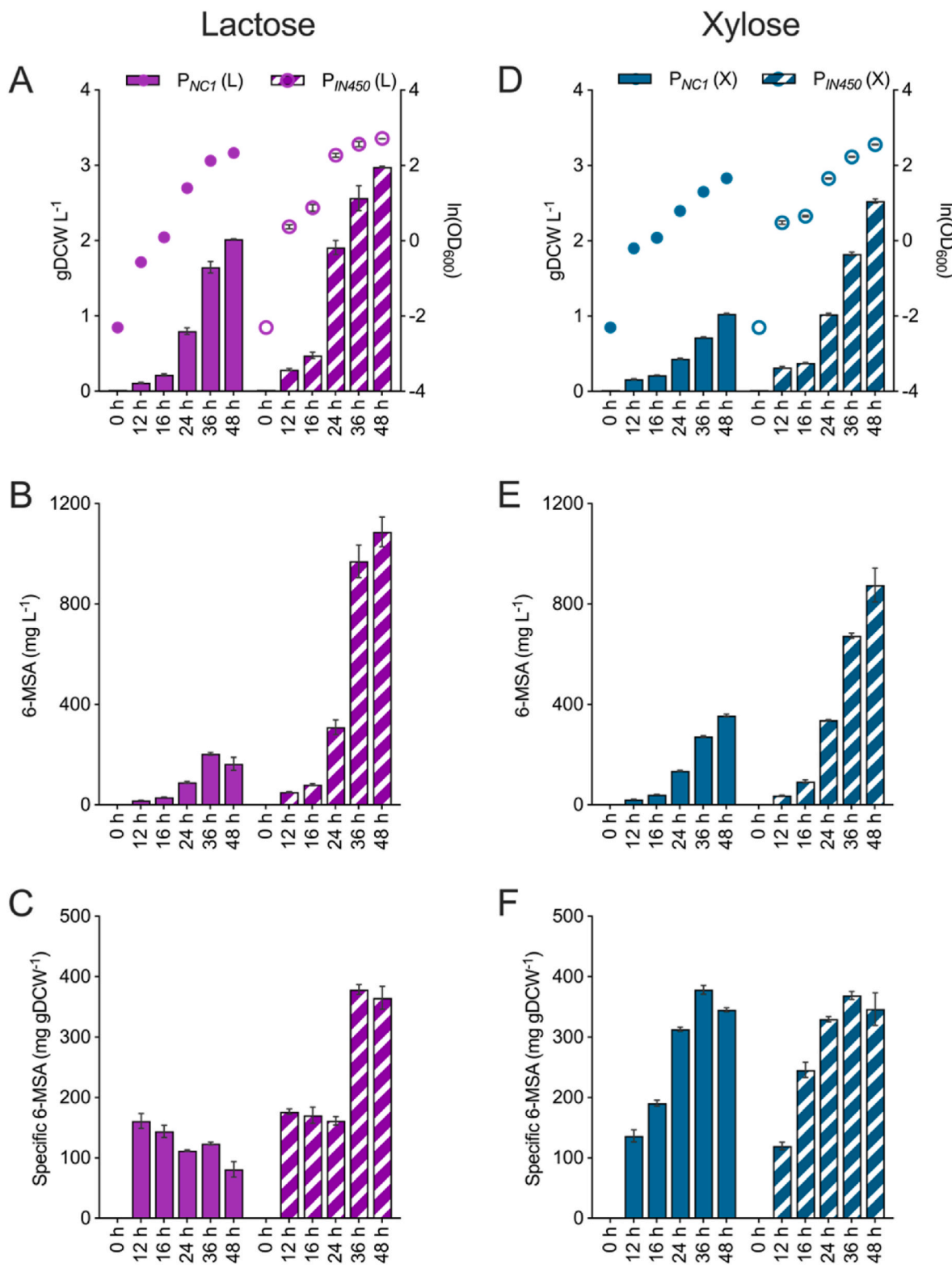


Fig. 5. Characterizing carbon-responsiveness for 6-MSA production in xylose and lactose media. Cell cultures were inoculated to an optical density of 0.1 at time 0, and cell densities (A, D), absolute 6-MSA titers (B, E), and specific titers (C, F) were measured after 12, 16, 24, 36, and 48 h of growth at 30 °C in 1% lactose (purple groups) or xylose (teal groups) media for *K. marxianus* strains expressing 6-MSAS under either P_{NC1} (solid bars) or P_{IN450} (striped bars) promoters. Growth curves (circles) in Panel A are plotted on the right y-axis while gDCW/L cell densities are plotted on the left axis. P_{IN450} behaves like a carbon-responsive promoter in lactose and a growth-associated promoter in xylose. Bars and scatter plots represent mean values \pm one SEM with $n = 3$. (For interpretation of the references to colour in this figure legend, the reader is referred to the Web version of this article.)

cosmetics industries and are known to be difficult to produce via microbial hosts, the plant hormone indole-acetic acid (IAA) and the monoterpene sabinene.

IAA is the most common auxin-class phytohormone, playing a major role in multiple plant cell processes. High levels of IAA impose growth inhibitory effects, making it an ideal candidate as a bioherbicide (Bunsangiam et al., 2021; Nicastro et al., 2021). One pathway for IAA biosynthesis is via tryptophan: the IaaM-encoding tryptophan-2-monoxygenase converts tryptophan to the indole intermediate indole-3-acetamide, which then gets converted to IAA by the IaaH-encoding indole-acetamide hydrolase (Fig. 6A). Bioproduction in yeast, however, can be quite challenging. Previous work has demonstrated IAA levels as low as ~9 mg/L (50 μ M) induces filamentous growth in *S. cerevisiae* (Prusty et al., 2004); the half-maximal inhibitory concentration (IC_{50}) was observed at ~100 mg/L (0.6 mM), and concentrations exceeding 175 mg/L (1 mM) completely arrested growth (Nicastro et al., 2021). IAA was found to interact with the target of rapamycin complex 1 (TORC1), a major regulatory node in eukaryotic growth. Interestingly, IAA synthesis and intracellular accumulation is possible upon entry into stationary phase; results from Nicastro et al. suggest that the accumulation of IAA aids in the transition of *S. cerevisiae* into quiescence because of its interaction with TORC1 (Nicastro et al., 2021).

We observed similar trends in *K. marxianus* and with significantly greater sensitivity to IAA than previously reported for *S. cerevisiae*. As low as 10 mg/L supplementation is enough to completely arrest *K. marxianus* growth (Figure S6). When cells are allowed to grow in the absence of IAA through exponential phase followed by IAA

supplementation, we see no reduction in *K. marxianus* growth; cell densities are either maintained or increased through 48 h (Figure S7), indicating IAA exhibits a microstatic effect on this yeast that inhibits initial proliferation, consistent with previous findings in *S. cerevisiae*.

The use of a strong promoter most active during quiescence is thus powerful for production of IAA in yeast. Here, we expressed the two enzymes IaaM and IaaH from *Pseudomonas savastanoi* in CBS712 Δ UAK from a single multi-copy bicistronic plasmid, with both genes under the control of either P_{NC1} or P_{IN450} . Transformed strains were cultured overnight in 1% lactose medium followed by reinoculation into medium supplemented with exogenous tryptophan, a 72-h culture period at 37 °C, and finally collection of supernatant samples for analysis by HPLC. Final cell densities were again higher with P_{IN450} compared to P_{NC1} (Fig. 6B), similar to what we observed for 6-MSA synthesis. Both 6-MSA and IAA are much more toxic to *K. marxianus* than TAL, and the use of the carbon-responsive promoter may allow better growth. Both absolute and specific IAA titers increased substantially with the hybrid promoter: 3.6-fold ($p < 0.001$) and 2.6-fold ($p < 0.001$), respectively (Fig. 6B). We also followed IAA levels with time (0–72 h) (Figure S8), given that IAA may not be detectable during exponential phase due to IAA interaction with TORC1. Consistent with the previous IAA-TORC1 interaction studies (Nicastro et al., 2021), no IAA was detected while the strains were still in exponential phase; the first instance of IAA detection coincides with stationary phase. Production using P_{NC1} results in a single increase in IAA production at 48 h, while P_{IN450} results in substantial increases at both 48 and 72 h, consistent with its carbon-responsive behavior (Figure S8). To our knowledge, this is the first attempt at producing IAA in minimal defined media, and the first instance of IAA

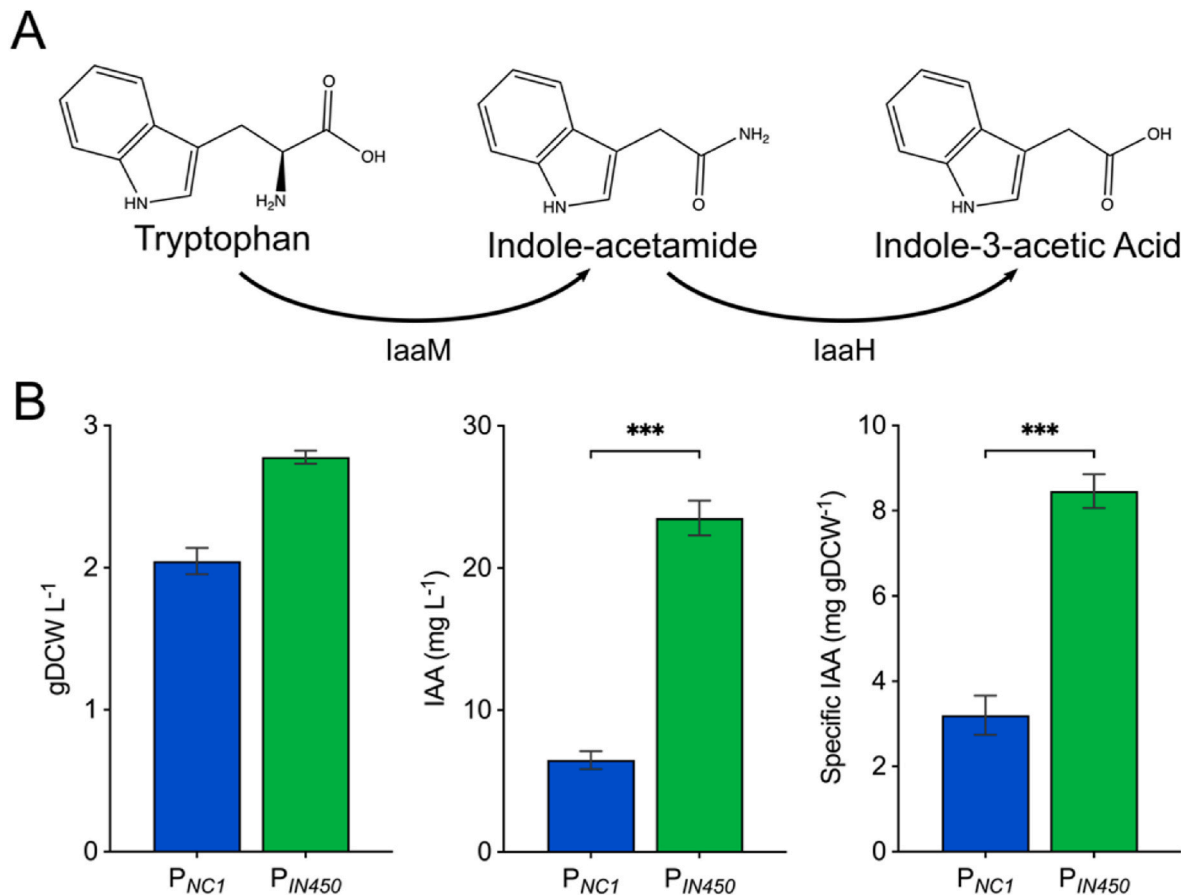


Fig. 6. Carbon-responsive promoter improves production of the toxic metabolite IAA. (A) Simplified pathway schematic for IAA biosynthesis from native tryptophan. (B) Cell densities, absolute IAA titers, and specific IAA titers after 48 h in lactose media supplemented with exogenous tryptophan for CBS712 Δ UAK expressing the IaaM and IaaH proteins from a multi-copy plasmid under control of either P_{NC1} (blue) or P_{IN450} (green). Bars represent mean values \pm one SEM, $n = 3$, *** $p < 0.001$. (For interpretation of the references to colour in this figure legend, the reader is referred to the Web version of this article.)

biosynthesis in *K. marxianus*.

We similarly evaluated the production of the toxic monoterpene sabinene. Sabinene is used in the flavor and fragrance industries due to its pleasant odor, as well as the pharmaceutical industry for its antimicrobial, antioxidant, and anti-inflammatory properties (Wang et al., 2021). Sabinene is a bicyclic C10 lipophilic compound formed by the isomerization and cyclization of geranyl pyrophosphate (GPP) via a sabinene synthase (Fig. 7A). Like most monoterpenes, sabinene exhibits toxicity to microbes by interfering with cell membrane properties (Brennan et al., 2012); to mitigate toxicity limitations and improve titers, *in situ* extraction with an organic overlay that traps the volatile monoterpene (Bureau et al., 2023; Ignea et al., 2019; Jia et al., 2020) is typically used. We expressed the *SabS1*-encoded sabinene synthase from *Salvia pomifera* (Ignea et al., 2014) under *P_{NC1}* or *P_{IN450}* control in CBS712ΔUAK. Transformants were grown overnight in 1% lactose and xylose media, followed by inoculation into fresh media with a 10% v/v IPM overlay to extract sabinene *in situ*. Strains were cultured for 48 h at 30 °C, followed by phase separation and analysis of the organic phase by GC-FID. In lactose, we observed a 2-fold increase both in absolute and specific titers with *P_{IN450}* compared to *P_{NC1}* ($p < 0.001$). Interestingly, we observe an even higher sabinene titer after 48 h in xylose, reaching 1.5 ± 0.2 mg/L (Figure S9), despite being a growth-associated promoter in xylose. Terpenoid generation via the mevalonate pathway results in a net generation of NADPH (Cao et al., 2018); because xylose metabolism is NADPH-dependent, the coupling of these two pathways allows for cofactor recycling, likely making production in xylose more favored than production in lactose. This is to our knowledge the first report of terpenoid production in *K. marxianus*, and with sabinene titers comparable to those in *S. cerevisiae* after extensive strain engineering (Ignea et al., 2014). These results further highlight the enhanced strength of our hybrid promoter, improving production of a wide range of compounds.

4. Conclusions

In this work, we designed and evaluated a set of hybrid promoters for the development of a novel carbon source responsive promoter for *K. marxianus*. We identified the hybrid *P_{IN450}* to be exceptionally strong in lactose; this promoter exhibited both partial repression during log phase and significant activation once the cells entered stationary phase, validated through fluorescence signaling and TAL production. High level expression of 2-PS under the control of *P_{IN450}* improved TAL titers and yield by 50% over the native *NC1* promoter alone, while rational promoter engineering further increased promoter strength. Use of this synthetic promoter improved production of the toxic polyketide 6-MSA 6.6-fold to 1.09 g/L, the highest 6-MSA titer from *K. marxianus* to date. Finally, by expressing the IaaM and IaaH proteins and the *S. pomifera* sabinene synthase protein under the control of *P_{IN450}*, we were able to increase both IAA and sabinene titers by over 2-fold each. Here, we reached sabinene titers of 0.67 and 1.5 mg/L in lactose and xylose, respectively, without strain or protein engineering. This carbon-responsive promoter adds to the growing yeast toolbox for *K. marxianus* strain engineering, further advancing this non-conventional yeast as a suitable candidate for industrial biomanufacturing.

CRediT authorship contribution statement

Shane Bassett: Conceptualization, Formal analysis, Investigation, Methodology, Writing – original draft, Writing – review & editing. **Nancy A. Da Silva:** Conceptualization, Formal analysis, Funding acquisition, Project administration, Supervision, Writing – review & editing.

Declaration of competing interest

The authors declare that they have no known competing financial

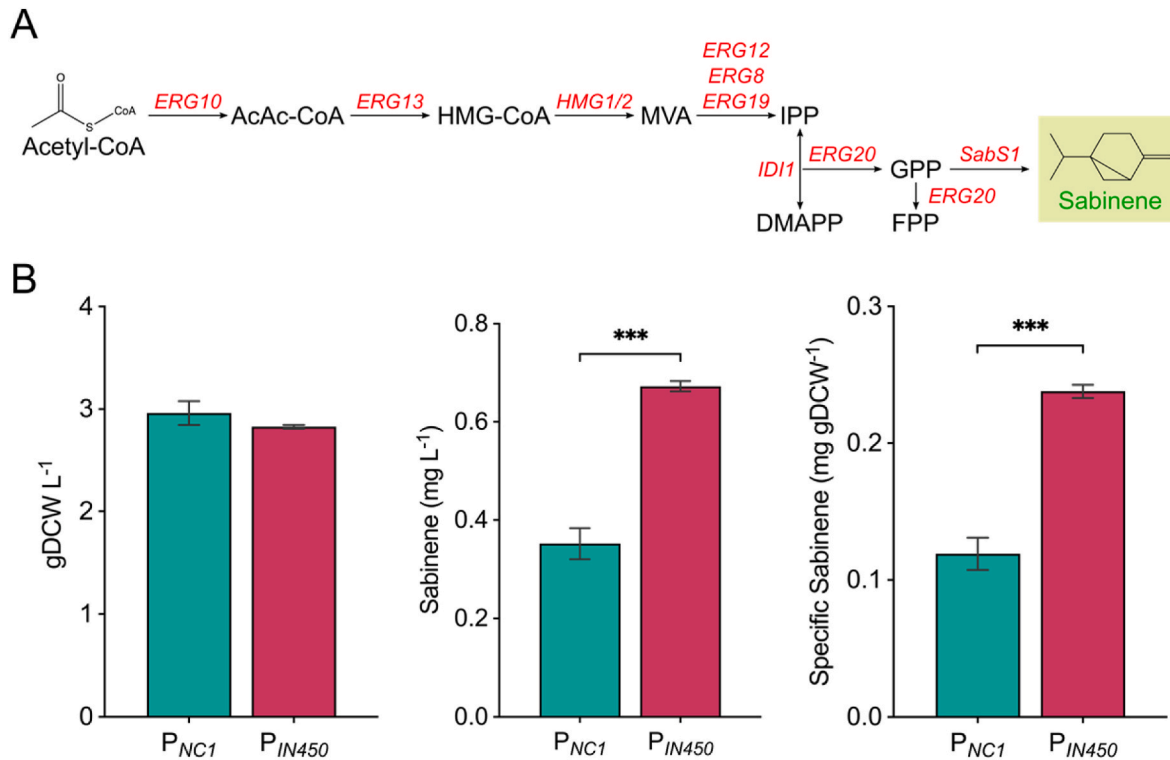


Fig. 7. Hybrid promoter increased the production of monoterpenes. (A) The monoterpene sabinene is a downstream product from the mevalonate pathway. (B) Cell densities, absolute sabinene titers, and specific sabinene titers were measured for CBS712ΔUAK transformed to express the *S. pomifera* *SabS1* from a multi-copy plasmid under control of either *P_{NC1}* (teal) or *P_{IN450}* (maroon) after 48 h of culture in lactose media. Bars represent mean values \pm one SEM, $n = 3$, *** $p < 0.001$.

interests or personal relationships that could have appeared to influence the work reported in this paper.

The author is an Editor-in-Chief for Metabolic Engineering Communications and was not involved in the editorial review or the decision to publish this article.

Data availability

Data will be made available on request.

Acknowledgements

This research was supported by the National Science Foundation (Grant No. CBET-1803677 and CBET-2225877). The authors thank Dr. William Black at UCI for assistance with GC-FID analyses, and Tharini Siddappa for initial IAA plasmid construction.

Appendix A. Supplementary data

Supplementary data to this article can be found online at <https://doi.org/10.1016/j.mec.2024.e00238>.

References

Bever, D., Wheeldon, I., Da Silva, N., 2022. RNA polymerase II-driven CRISPR-Cas9 system for efficient non-growth-biased metabolic engineering of *Kluyveromyces marxianus*. *Metabolic Engineering Communications*, e00208. <https://doi.org/10.1016/j.mec.2022.e00208>.

Bever-Sneary, D., 2023. *Development and Application of CRISPR-Cas9 Tools for Metabolic Engineering in K. Marxianus towards Enhanced Polyketide Biosynthesis*. University of California, Irvine.

Brennan, T.C.R., Turner, C.D., Krömer, J.O., Nielsen, L.K., 2012. Alleviating monoterpene toxicity using a two-phase extractive fermentation for the bioproduction of jet fuel mixtures in *Saccharomyces cerevisiae*. *Biotechnol. Bioeng.* <https://doi.org/10.1002/bit.24536>.

Breunig, K.D., Bolotin-Fukuhara, M., Bianchi, M.M., Bourgarel, D., Falcone, C., Ferrero, I., Frontali, L., Goffrini, P., Krijger, J.J., Mazzoni, C., Milkowski, C., Steensma, H.Y., Węsoliowski-Louvel, M., Zeeman, A.M., 2000. Regulation of primary carbon metabolism in *Kluyveromyces lactis*. In: *Enzyme and Microbial Technology*. [https://doi.org/10.1016/S0141-0229\(00\)00170-8](https://doi.org/10.1016/S0141-0229(00)00170-8).

Bunsangiam, S., Thongpae, N., Limtong, S., Srisuk, N., 2021. Large scale production of indole-3-acetic acid and evaluation of the inhibitory effect of indole-3-acetic acid on weed growth. *Sci. Rep.* 11, 13094. <https://doi.org/10.1038/s41598-021-92305-w>.

Bureau, J.-A., Oliva, M.E., Dong, Y., Ignea, C., 2023. Engineering yeast for the production of plant terpenoids using synthetic biology approaches. *Nat. Prod. Rep.* 40, 1822–1848. <https://doi.org/10.1039/D3NP00005B>.

Cao, Y., Zhang, H., Liu, H., Liu, W., Zhang, R., Xian, M., Liu, Huizhou, 2018. Biosynthesis and production of sabenine: current state and perspectives. *Appl. Microbiol. Biotechnol.* 102, 1535–1544. <https://doi.org/10.1007/s00253-017-8695-5>.

Cardenas, J., Da Silva, N.A., 2014. Metabolic engineering of *Saccharomyces cerevisiae* for the production of triacetic acid lactone. *Metab. Eng.* <https://doi.org/10.1016/j.ymben.2014.07.008>.

Choi, J.W., 2014. *Engineering of Yeast for the Production of Fuels and Polyketides*. University of California, Irvine.

Choi, J.W., Da Silva, N.A., 2014. Improving polyketide and fatty acid synthesis by engineering of the yeast acetyl-CoA carboxylase. *J. Biotechnol.* 187, 56–59. <https://doi.org/10.1016/j.jbiotec.2014.07.430>.

Da Silva, N.A., Srikrishnan, S., 2012. Introduction and expression of genes for metabolic engineering applications in *Saccharomyces cerevisiae*. *FEMS Yeast Res.* 12, 197–214. <https://doi.org/10.1111/j.1567-1364.2011.00769.x>.

Dusseaux, S., Wajn, W.T., Liu, Y., Ignea, C., Kampranis, S.C., 2020. Transforming yeast peroxisomes into microfactories for the efficient production of high-value isoprenoids. *Proc. Natl. Acad. Sci. U.S.A.* <https://doi.org/10.1073/pnas.2013968117>.

Fonseca, G.G., De Carvalho, N.M.B., Gombert, A.K., 2013. Growth of the yeast *Kluyveromyces marxianus* CBS 6556 on different sugar combinations as sole carbon and energy source. *Appl. Microbiol. Biotechnol.* <https://doi.org/10.1007/s00253-013-4748-6>.

Fonseca, G.G., Heinzel, E., Wittmann, C., Gombert, A.K., 2008. The yeast *Kluyveromyces marxianus* and its biotechnological potential. *Appl. Microbiol. Biotechnol.* <https://doi.org/10.1007/s00253-008-1458-6>.

Gomes, E.S., Schuch, V., Lemos, E.G. de M., 2013. Biotechnology of polyketides: new breath of life for the novel antibiotic genetic pathways discovery through metagenomics. *Braz. J. Microbiol.* 44, 1007–1034. <https://doi.org/10.1590/S1517-83822013000400002>.

Groeneweld, P., Stouthamer, A.H., Westerhoff, H.V., 2009. Super life - how and why "cell selection" leads to the fastest-growing eukaryote. *FEBS J.* <https://doi.org/10.1111/j.1742-4658.2008.06778.x>.

Hitschler, J., Boles, E., 2019. De novo production of aromatic m-cresol in *Saccharomyces cerevisiae* mediated by heterologous polyketide synthases combined with a 6-methylsalicylic acid decarboxylase. *Metabolic Engineering Communications* 9, e00093. <https://doi.org/10.1016/j.mec.2019.e00093>.

Ignea, C., Pontini, M., Maffei, M.E., Makris, A.M., Kampranis, S.C., 2014. Engineering monoterpene production in yeast using a synthetic dominant negative geranyl diphosphate synthase. *ACS Synth. Biol.* <https://doi.org/10.1021/sb400115e>.

Ignea, C., Raadam, M.H., Motawia, M.S., Makris, A.M., Vickers, C.E., Kampranis, S.C., 2019. Orthogonal monoterpenoid biosynthesis in yeast constructed on an isomeric substrate. *Nat. Commun.* 10, 3799. <https://doi.org/10.1038/s41467-019-11290-x>.

Jia, H., Chen, T., Qu, J., Yao, M., Xiao, W., Wang, Y., Li, C., Yuan, Y., 2020. Collaborative subcellular compartmentalization to improve GPP utilization and boost sabinene accumulation in *Saccharomyces cerevisiae*. *Biochem. Eng. J.* <https://doi.org/10.1016/j.bej.2020.107768>.

Jongedijk, E., Cankar, K., Buchhaupt, M., Schrader, J., Bouwmeester, H., Beekwilder, J., 2016. Biotechnological production of limonene in microorganisms. *Appl. Microbiol. Biotechnol.* <https://doi.org/10.1007/s00253-016-7337-7>.

Kampranis, S.C., Makris, A.M., 2012. Developing a yeast cell factory for the production of terpenoids. *Comput. Struct. Biotechnol. J.* <https://doi.org/10.5936/csb.201210006>.

Karim, A., Gerlani, N., Aider, M., 2020. *Kluyveromyces marxianus*: an emerging yeast cell factory for applications in food and biotechnology. *Int. J. Food Microbiol.* <https://doi.org/10.1016/j.ijfoodmicro.2020.108818>.

Kealey, J.T., Liu, L., Santi, D.V., Betlach, M.C., Barr, P.J., 1998. Production of a polyketide natural product in nonpolyketide-producing prokaryotic and eukaryotic hosts. *Proceedings of the National Academy of Sciences of the United States of America*. <https://doi.org/10.1073/pnas.95.2.505>.

Kumar, P., Sahoo, D.K., Sharma, D., 2021. The identification of novel promoters and terminators for protein expression and metabolic engineering applications in *Kluyveromyces marxianus*. *Metabolic Engineering Communications*. <https://doi.org/10.1016/j.mec.2020.e00160>.

Lacour, S., Landini, P., 2004. σS-Dependent gene expression at the onset of stationary phase in *Escherichia coli*: function of σS-dependent genes and identification of their promoter sequences. *J. Bacteriol.* 186, 7186–7195. <https://doi.org/10.1128/jb.186.21.7186-7195.2004>.

Lane, M.M., Morrissey, J.P., 2010. *Kluyveromyces marxianus*: a yeast emerging from its sister's shadow. *Fungal Biology Reviews* 24, 17–26. <https://doi.org/10.1016/j.fbr.2010.01.001>.

Lang, X., Besada-Lombana, P.B., Li, M., Da Silva, N.A., Wheeldon, I., 2020. Developing a broad-range promoter set for metabolic engineering in the thermotolerant yeast *Kluyveromyces marxianus*. *Metabolic Engineering Communications*. <https://doi.org/10.1016/j.mec.2020.e00145>.

Lee, K.K.M., Da Silva, N.A., Kealey, J.T., 2009. Determination of the extent of phosphopantetheinylation of polyketide synthases expressed in *Escherichia coli* and *Saccharomyces cerevisiae*. *Anal. Biochem.* 394, 75–80. <https://doi.org/10.1016/j.ab.2009.07.010>.

Lertwattanasakul, N., Kosaka, T., Hosoyama, A., Suzuki, Y., Rodruessamee, N., Matsutani, M., Murata, M., Fujimoto, N., Suprayogi, Tsuchikane, K., Limtong, S., Fujita, N., Yamada, M., 2015. Genetic basis of the highly efficient yeast *Kluyveromyces marxianus*: complete genome sequence and transcriptome analyses. *Biotechnol. Biofuels*. <https://doi.org/10.1186/s13068-015-0227-x>.

Li, M., Lang, X., Moran Cabrera, M., De Keyser, S., Sun, X., Da Silva, N., Wheeldon, I., 2021. CRISPR-mediated multigene integration enables Shikimate pathway refactoring for enhanced 2-phenylethanol biosynthesis in *Kluyveromyces marxianus*. *Biotechnol. Biofuels*. <https://doi.org/10.1186/s13068-020-01852-3>.

Li, Mengwan, 2022. *CRISPR/Cas9-Enabled Functional Genomic Editing in the Thermotolerant Yeast Kluyveromyces Marxianus*. UC Riverside.

Light, R.J., 1967. The biosynthesis of 6-methylsalicylic acid. *J. Biol. Chem.* 242, 1880–1886. [https://doi.org/10.1016/S0021-9258\(18\)96083-7](https://doi.org/10.1016/S0021-9258(18)96083-7).

Liscum, L., Finer-Moore, J., Stroud, R.M., Luskey, K.L., Brown, M.S., Goldstein, J.L., 1985. Domain structure of 3-hydroxy-3-methylglutaryl coenzyme A reductase, a glycoprotein of the endoplasmic reticulum. *J. Biol. Chem.* [https://doi.org/10.1016/s0021-9258\(18\)89764-2](https://doi.org/10.1016/s0021-9258(18)89764-2).

Liu, L., Bao, W., Men, X., Zhang, H., 2022. Engineering for life in toxicity: key to industrializing microbial synthesis of high energy density fuels. *Engineering Microbiology*. <https://doi.org/10.1016/j.engm.2022.100013>.

Löbs, A.K., Engel, R., Schwartz, C., Flores, A., Wheeldon, I., 2017. CRISPR-Cas9-enabled genetic disruptions for understanding ethanol and ethyl acetate biosynthesis in *Kluyveromyces marxianus*. *Biotechnol. Biofuels*. <https://doi.org/10.1186/s13068-017-0854-5>.

López, M.L., Redruello, B., Valdés, E., Moreno, F., Heinisch, J.J., Rodicio, R., 2004. Isocitrate lyase of the yeast *Kluyveromyces lactis* in subject to glucose repression but not to catabolite inactivation. *Curr. Genet.* <https://doi.org/10.1007/s00294-003-0453-9>.

Markham, K.A., Palmer, C.M., Chwatk, M., Wagner, J.M., Murray, C., Vazquez, S., Swaminathan, A., Chakravarty, I., Lynd, N.A., Alper, H.S., 2018. Rewiring *Yarrowia lipolytica* toward triacetic acid lactone for materials generation. *Proceedings of the National Academy of Sciences*. <https://doi.org/10.1073/pnas.1721203115>.

McTaggart, T.L., Bever, D., Bassett, S., Da Silva, N.A., 2019. Synthesis of polyketides from low cost substrates by the thermotolerant yeast *Kluyveromyces marxianus*. *Biotechnol. Bioeng.* <https://doi.org/10.1002/bit.26976>.

Nicastro, R., Raucci, S., Michel, A.H., Stumpe, M., Osuna, G.M.G., Jaquenoud, M., Kornmann, B., Virgilio, C.D., 2021. Indole-3-acetic acid is a physiological inhibitor of TORC1 in yeast. *PLoS Genet.* 17, e1009414. <https://doi.org/10.1371/journal.pgen.1009414>.

Pfeifer, B.A., Khosla, C., 2001. Biosynthesis of polyketides in heterologous hosts. *Microbiol. Mol. Biol. Rev.* <https://doi.org/10.1128/mmbr.65.1.106-118.2001>.

Prusty, R., Grisafi, P., Fink, G.R., 2004. The plant hormone indoleacetic acid induces invasive growth in *Saccharomyces cerevisiae*. *Proc. Natl. Acad. Sci. USA* 101, 4153–4157. <https://doi.org/10.1073/pnas.0400659101>.

Rajkumar, A.S., Varela, J.A., Juergens, H., Daran, J.M.G., Morrissey, J.P., 2019. Biological parts for *Kluyveromyces marxianus* synthetic biology. *Front. Bioeng. Biotechnol.* <https://doi.org/10.3389/fbioe.2019.00097>.

Ricci, A., Allende, A., Bolton, D., Chemaly, M., Davies, R., Girones, R., Koutsoumanis, K., Lindqvist, R., Nörrung, B., Robertson, L., Ru, G., Fernández Escámez, P.S., Sanaa, M., Simmons, M., Skandamis, P., Snary, E., Speybroeck, N., Ter Kuile, B., Threlfall, J., Wahlström, H., Cocconcelli, P.S., Peixe, L., Maradona, M.P., Querol, A., Suarez, J.E., Sundh, I., Vlak, J., Barizzone, F., Correia, S., Herman, L., 2018. Update of the list of QPS-recommended biological agents intentionally added to food or feed as notified to EFSA 7: suitability of taxonomic units notified to EFSA until September 2017. *EFSA J.* <https://doi.org/10.2903/j.efsa.2018.5131>.

Rodicio, R., López, M.L., Cuadrado, S., Cid, A.F., Redruello, B., Moreno, F., Heinisch, J.J., Hegewald, A.K., Breunig, K.D., 2008. Differential control of isocitrate lyase gene transcription by non-fermentable carbon sources in the milk yeast *Kluyveromyces lactis*. *FEBS (Fed. Eur. Biochem. Soc.) Lett.* <https://doi.org/10.1016/j.febslet.2008.01.017>.

Romanos, M.A., Scorer, C.A., Clare, J.J., 1992. Foreign gene expression in yeast: a review. *Yeast* 8. <https://doi.org/10.1002/yea.320080602>.

Sakhtah, H., Behler, J., Ali-Reynolds, A., Causey, T.B., Vainauskas, S., Taron, C.H., 2019. A novel regulated hybrid promoter that permits autoinduction of heterologous protein expression in *Kluyveromyces lactis*. *Appl. Environ. Microbiol.* <https://doi.org/10.1128/AEM.00542-19>.

Spencer, J.B., Jordan, P.M., 1992. Purification and properties of 6-methylsalicylic acid synthase from *Penicillium patulum*. *Biochem. J.* 288, 839–846. <https://doi.org/10.1042/bj2880839>.

Varela, J.A., Puricelli, M., Ortiz-Merino, R.A., Giacomobono, R., Braun-Galleani, S., Wolfe, K.H., Morrissey, J.P., 2019. Origin of lactose fermentation in *Kluyveromyces lactis* by interspecies transfer of a neo-functionalized gene cluster during domestication. *Curr. Biol.* <https://doi.org/10.1016/j.cub.2019.10.044>.

Vickery, C.R., Cardenas, J., Bowman, M.E., Burkart, M.D., Da Silva, N.A., Noel, J.P., 2018. A coupled in vitro/in vivo approach for engineering a heterologous type III PKS to enhance polyketide biosynthesis in *Saccharomyces cerevisiae*. *Biotechnol. Bioeng.* <https://doi.org/10.1002/bit.26564>.

Wang, Z., Zhang, R., Yang, Q., Zhang, J., Zhao, Y., Zheng, Y., Yang, J., 2021. Chapter One - recent advances in the biosynthesis of isoprenoids in engineered *Saccharomyces cerevisiae*. In: Gadd, G.M., Sariaslani, S. (Eds.), *Advances in Applied Microbiology*. Academic Press, pp. 1–35. <https://doi.org/10.1016/bs.aams.2020.11.001>.

Wattanachaisaereekul, S., Lantz, A.E., Nielsen, M.L., Andrésson, Ö.S., Nielsen, J., 2007. Optimization of heterologous production of the polyketide 6-MSA in *Saccharomyces cerevisiae*. *Biotechnol. Bioeng.* <https://doi.org/10.1002/bit.21286>.

Wattanachaisaereekul, S., Lantz, A.E., Nielsen, M.L., Nielsen, J., 2008. Production of the polyketide 6-MSA in yeast engineered for increased malonyl-CoA supply. *Metab. Eng.* 10, 246–254. <https://doi.org/10.1016/j.ymben.2008.04.005>.

Weinhandl, K., Winkler, M., Glieder, A., Camattari, A., 2014. Carbon source dependent promoters in yeasts. *Microb. Cell Factories*. <https://doi.org/10.1186/1475-2859-13-5>.

Weissman, K.J., 2009. Chapter 1 introduction to polyketide biosynthesis. *Methods Enzymol.* 459, 3–16. [https://doi.org/10.1016/S0076-6879\(09\)04601-1](https://doi.org/10.1016/S0076-6879(09)04601-1).

Yang, C., Hu, S., Zhu, S., Wang, D., Gao, X., Hong, J., 2015. Characterizing yeast promoters used in *Kluyveromyces marxianus*. *World J. Microbiol. Biotechnol.* <https://doi.org/10.1007/s11274-015-1899-x>.

Yu, J., Landberg, J., Shavarebi, F., Bilanchone, V., Okerlund, A., Wanninayake, U., Zhao, L., Kraus, G., Sandmeyer, S., 2018. Bioengineering triacetic acid lactone production in *Yarrowia lipolytica* for pogostone synthesis. *Biotechnol. Bioeng.* <https://doi.org/10.1002/bit.26733>.

Yu, X., Xu, J., Liu, X., Chu, X., Wang, P., Tian, J., Wu, N., Fan, Y., 2015. Identification of a highly efficient stationary phase promoter in *Bacillus subtilis*. *Sci. Rep.* 5, 18405. <https://doi.org/10.1038/srep18405>.

Yu, Y., Mo, W., Ren, H., Yang, X., Lu, W., Luo, T., Zeng, J., Zhou, J., Qi, J., Lu, H., 2021. Comparative genomic and transcriptomic analysis reveals specific features of gene regulation in *Kluyveromyces marxianus*. *Front. Microbiol.* 12.

Zhang, Y., Nielsen, J., Liu, Z., 2017. Engineering yeast metabolism for production of terpenoids for use as perfume ingredients, pharmaceuticals and biofuels. *FEMS Yeast Res.* <https://doi.org/10.1093/femsyr/fox080>.